J. Synchrotron Rad. (1998). **5**, 820–822

Ray-tracing analysis of capillary concentrators for macromolecular crystallography

Daniel J. Thiel

Department of Biochemistry, Molecular and Cell Biology, Cornell University, Ithaca, NY 14853, USA.
E-mail: djt7@cornell.edu

(*Received 4 August 1997; accepted 14 October 1997*)

The use of capillary concentrators as X-ray condensers specifically for macromolecular X-ray diffraction experiments using synchrotron radiation is evaluated. Monocapillary and polycapillary designs are assessed by ray-tracing analysis to evaluate how effectively these capillary concentrators can increase the X-ray intensity onto a 50 μm crystal.

Keywords: capillary optics; ray tracing; X-ray focusing.

1. Introduction

At third-generation sources, conventional X-ray optics should be able to produce small focused incident beams. However, at first- and second-generation sources, larger source sizes benefit from the use of other approaches.

In this report, ray-tracing analysis is used to analyze two types of single-stranded tapered capillary concentrators – the single-bore monocapillary and the multibore polycapillary. The objective of this investigation is twofold: to evaluate how effectively these capillary concentrators can increase the X-ray intensity onto a 50 μm macromolecular crystal as compared with a collimator, and to determine which type of capillary concentrator (polycapillary or monocapillary) will produce the greater increase in intensity in such a spot.

2. Capillary concentrators

X-ray capillary optics based on total reflection fall into two categories: focusing optics and concentrators. A focusing capillary is a single-bounce device. For a point source, such a device has an ellipsoidal figure, by definition. It has been shown for a synchrotron source of finite size that focusing capillaries may be attained by truncating the optic several centimeters upstream of the focus (Balaic *et al.*, 1995). Of course, not all of the incident rays are focused to the focal spot since a truncated segment fails to capture all of the rays. In addition, slight deviations of the figure can compromise the focusing performance.

Capillary concentrators, on the other hand, do not have stringent design specifications. A concentrator is a multiple-bounce device; therefore, there is greater flexibility in designing such optics. For example, one idea for forming X-ray concentrators is to assemble many strands of multi-channel glass capillaries into large arrays where each channel is essentially aimed at the same exit point (Kumakhov, 1990). This approach has been applied to conventional X-ray sources. In this report, we analyze the performance of two types of X-ray concentrators which have been implemented at synchrotron sources – tapered monocapillaries and tapered polycapillaries.

Tapered monocapillary concentrators may have any taper profile; however, the ideal figure is still the ellipse. An elliptically tapered concentrator is identical to the focusing capillary described above except that the element may be extended within a few microns of the focal position leading to a smaller diameter opening. As shown in this report, the advantage of this is that all incident rays may be directed to the small opening. A two-dimensional schematic diagram of a ray propagating down an ellipsoidal concentrator is shown in Fig. 1.

Tapered polycapillary concentrators are formed from glass tubing composed of many small axial channels. The polycapillary tubing which appears most promising for macromolecular concentrators is hexagonal-shaped and consists of 336 channels, each 16 μm in diameter, where the outer dimension of the tubing is 460 μm wide (Hoffman *et al.*, 1994). Fig. 2 shows a cross-sectional schematic diagram of such a concentrator.

Tapered concentrators may produce small condensed X-ray beams defined by the small opening at their tips; however, these beams may have significant divergence because of the multiple reflections of some of the rays. Beam divergence must be considered to avoid overlap of diffraction spots.

3. Ray tracing

Analysis is performed using a computer code which calculates in two-dimensions the trajectories and transmission of the entering X-rays (Thiel, 1992). The program uses a zero-finding routine to calculate points of intersection between a defined ray and the reflecting surface. All rays are treated as meridional rays, rays which remain in the same plane as they propagate down the bore.

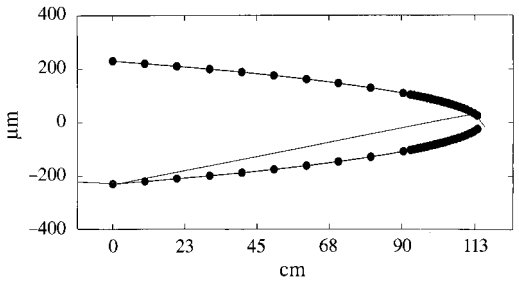

Figure 1
Cross section of an ellipsoidal monocapillary concentrator. The trajectory of the extremum ray which undergoes two reflections before exiting the small tip is shown.

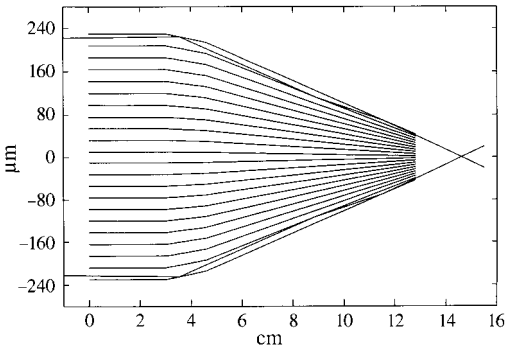

Figure 2
Cross section of a polycapillary concentrator. Rays are shown propagating through the outer channels and being directed to the 'focal spot' located 2 cm from the tip.

Table 1
Monocapillary performance with unfocused radiation.

Mono-capillary	Length (cm)	α_i (mrad)	Source size (mm)	T (%)	$\lvert\theta_o\rvert$ (mrad)
*e*5	113	0.05	1.0	99.5	1.76
		0.2	5.5	99.0	1.78
		0.35	10.0	16.2	3.82
		0.5	14.5	0	–
		0.7	20.5	0	–
*e*6	551	0.05	1.0	99.7	0.72
		0.2	5.5	97.2	1.93
		0.35	10.0	21.2	3.23
		0.5	14.5	0	–
		0.7	20.5	0	–
*e*21	186	0.05	1.0	99.7	1.37
		0.2	5.5	99.2	1.75
		0.35	10.0	96.4	3.22
		0.5	14.5	3.0	4.70
		0.7	20.5	0	–

Furthermore, the reflectance of each bounce, which is a function of incidence angle, X-ray energy and the reflecting material, is calculated using the Fresnel equations. In this analysis, the value of the X-ray energy was chosen to be 12 keV and the material of the capillaries was SiO_2.

Systematic sampling of the incident rays, where a small number of rays are chosen, is used to evaluate the performance of the designs. Random sampling would require thousands of rays in order to make such a study meaningful. Systematic sampling is a valid approach here since the regions most efficiently and most inefficiently transporting X-rays are easily identified.

4. Unfocused beamlines

First, we consider the case of an unfocused beamline. For the monocapillary concentrator, the ideal taper is an ellipsoidal segment. (The defining ellipse has an eccentricity so close to unity that it can also be defined as a parabola where the focus lies just outside the tip of the capillary.) Capillary entrance and exit of 460 and 50 μm, respectively, were chosen along with a source distance of 15 m. Design parameters which were varied include the separation of the foci of the defining ellipse (therefore, the length of the capillary), the slope of the capillary wall at the tip, and the size of the source. The design optimization is summarized in Table 1, where a comparison of three ellipsoidal profiles is given. Transmission (T) of the worst-case (extremum) ray, that is, the ray that strikes the inner wall just at the entrance with the greatest angle of incidence, α_i, was calculated. From this analysis, we can determine how large the source may be while still expecting high transmission efficiency.

The first capillary, *e*5, is a portion of an ellipse with foci separated by 15 m. The slope at the tip was constrained to be 1 mrad and the capillary length 1.13 m. The second design, *e*6, involves a longer capillary, 5.51 m in length, displaying a more gradual slope of 0.3 mrad at the tip. The final design, *e*21, has a 1 mrad tip slope and a 4 m foci separation, thereby increasing its length beyond that of the first design to 1.86 m. With the slope at the tip restrained to 1 mrad or less, rays travelling undeflected from the source to the interior wall at the tip, where the taper angle is greatest, have a divergence angle of no greater than 2 mrad + α_i.

According to the ray-tracing results, for a source size of 5.5 mm or less, each design effectively transmits all entering rays.

Table 2
Polycapillary performance with unfocused radiation.

A total of N rays were traced of which n rays exited the concentrator.

Poly-capillary	Length (cm)	α_i (mrad)	Source size (mm)	n/N	T (%)	$\lvert\theta_o\rvert$ (mrad)
b	7.3	0.05	1.0	13/17	75.6	2.94
		0.2	5.5	12/17	67.9	2.80
		0.7	20.5	1/17	5.30	0.43
c	19.9	0.05	1.0	13/17	75.6	0.99
		0.2	5.5	9/17	47.2	1.96
		0.7	20.5	0/17	0	–

Increasing the source size to 10 mm results in a drop in transmission of the extremum ray below 25% for the first two capillary designs. For the third design, such a decrease occurs as the source size approaches 14.5 mm. Also given in Table 1 is the half-angle output divergence, θ_o, of the extremum ray. This parameter, along with crystal mosaicity and unit-cell size, contributes to overlap of diffraction spots. In general, we will consider half-angle divergences of greater than 2 mrad unacceptable. For a particular experiment, Table 1 may be used as a guide in aperturing the source.

Now we consider the polycapillary tubing. Unlike the monocapillary case only 60% of the X-rays striking the region defined by the 460 μm cross section enter the open channels due to occlusion by the interior glass walls. Another difference is that there is no well defined single extremum ray as in the monocapillary case. Since the outer channels of a tapered polycapillary transmit the X-rays the least efficiently of all the channels, in this analysis we focus on the outer channels.

To obtain a similar estimate as for the monocapillary case, we systematically launch 17 rays from the extreme edge of the source such that the rays enter the outer 16 μm wide channel over a grid where each ray is separated by 1 μm, thereby striking the inner wall at various locations with maximum incidence angle. Because the sampling is conducted systematically rather than randomly, the use of only 17 rays gives meaningful results. The results of two idealized polycapillary profiles which taper from 460 to 50 μm over two distinct taper zones are given in Table 2. The initial zone, defined as the region where the outer wall slopes 16 μm transversely so that all initial reflections occur in this region, must have a taper angle smaller than the critical angle. This is not the case for the second zone, as shown in Fig. 2. The first design is 7.3 cm long with an initial zone 1.1 cm long, and the second is 19.9 cm long with an initial zone 3.0 cm long; both polycapillary designs are considerably shorter than the monocapillaries mentioned above. As shown in Table 2, a source size greater than 5.5 mm leads to unacceptable beam divergence as well as low X-ray transmission.

The shorter capillary, which is similar to optics previously tested (Hoffman *et al.*, 1994), gives higher transmission; however, the divergence is too large for most macromolecular diffraction experiments. With increased length, the second design gives reasonable performance for a source size as large as 5.5 mm, and the divergence is similar to that of the second monocapillary listed in Table 1. Notice that the transmission of these designs never approaches that of the monocapillary. Further increasing the length reduces the divergence but also decreases the transmission. For the case of no additional focusing optics, we conclude that monocapillaries are superior in performance.

5. Focused beamlines

Next, we consider the case of the focused wiggler beamlines at CHESS. The X-ray beam is focused in both planes where horizontal focusing is achieved using a mechanically-bent metal-coated glass mirror, and vertical focusing is achieved by a bent-triangular Si(111) crystal. It has been determined that by roughening the face of the silicon monochromator a greater flux is achieved. Such optics are difficult to precisely model – to first order the beamline optics are imaging optics; however, in reality there is no well defined focus.

In our ray-tracing analysis, we incorporate the general parameters of the focusing optics, where the horizontal divergence has a FWHM of 1.4 mrad and the vertical divergence is 0.4 mrad. We assume that the entrance of the capillary is positioned within the beam waist and that it is uniformly illuminated by this full-angle divergence. Table 3 presents results from the five previous capillary designs plus one additional monocapillary and one additional polycapillary design. In each case, a total of 204 extremum rays were launched, 119 in the horizontal plane and 85 in the vertical, over a 1 μm grid over the 16 μm of the outer channel. At each of these 17 grid points, rays with incident divergence of 0, ±0.05, ±0.2 and ±0.7 mrad were launched to simulate the horizontal plane from the source. Rays with incident divergences of 0, ±0.05 and ±0.2 mrad were launched for the vertical.

The results represent lower limits for actual X-ray transmission. Again, the advantage of the monocapillaries over polycapillaries is shown. The extremum-ray transmission steadily increases as the monocapillary length decreases; however, the divergence becomes prohibitively large with the fourth design. The slope at the tip was increased to 2.5 mrad, so many non-extremum rays will also have prohibitively large divergence with this design. Polycapillaries also exhibit a reduction in divergence as the length is increased. Though not shown in the table, it is important to note that in the analysis of all of the profiles no rays with incident divergence of ±0.7 mrad were transmitted. Despite this, high transmissions were still obtained. For the existing protein crystallography beamlines at CHESS, the ideal design is monocapillary *e*5 due to its relatively short length, high transmission and low divergence.

Table 3
Capillary performance with focused radiation.

The initial taper zone of polycapillary d is 3.2 cm long.

Capillary	Length (cm)	T (%)	$\|\theta_o\|$ (mrad)
*e*5	113	83.1	1.01
*e*6	551	82.5	0.978
*e*21	186	83.0	1.32
*e*14	45	91.2	2.28
b	7.3	62.8	2.82
c	19.9	56.4	1.41
d	21.6	59.4	1.21

6. Conclusions

The monocapillary concentrators are longer and somewhat more cumbersome to implement; however, we conclude that they are the superior design for use on the macromolecular beamlines at CHESS. For unfocused radiation from a small source, the 5.51 m long design (*e*6) is preferable. As the source size increases to the extent that the incident divergence of the extremum ray is 0.35 mrad or greater, the *e*21 profile becomes favorable with respect to transmission; however, for this source size any profile (monocapillary or polycapillary) results in beam divergence too large for macromolecular crystallographic applications. For the CHESS focused beams, the monocapillary design, *e*5, is the optimal design. With a 50 μm sample, an increase in flux of almost two orders of magnitude is predicted. Slightly smaller gains are predicted using the optimized polycapillary design. In addition, with the polycapillary optics, the actual transmission will be further reduced by almost a factor of two due to the 40% closed area which was neglected in the ray-tracing analysis.

The result for the case of the focused CHESS beamlines warrants additional comments. The optimal concentrator described is able to collect the focused radiation over a 460 μm area and further condense the photons to a 50 μm spot. This is possible because the source size is large and the beamline focusing optics are not capable of truly focusing the beam. The gain due to the concentrator does not represent a violation of Liouville's Theorem of phase space conservation. Such a result would not be possible with a point source and ideal focusing optics.

This study was restricted to the proven macromolecular beamlines at CHESS where the source size is quite large (6.7 mm FWHM horizontally and 1.3 mm FWHM vertically). Surface roughness was not included in the modelling. Though it can be a significant factor in focusing capillaries, it has been shown that typical glass roughness is not a significant parameter for capillary concentrators (Wang *et al.*, 1996).

Tests are underway to determine the acceptable limits of beam divergence generated by these optics when applied to macromolecular crystallography. Preliminary protein diffraction results using a focusing capillary rather than a concentrator have been reported (Balaic *et al.*, 1996).

I thank Don Bilderback for many helpful discussions. This work was supported by the National Institutes of Health Grant No. RR-01646.

References

Balaic, D. X., Barnea, Z., Nugent, K. A., Garrett, R. F., Varghese, J. N. & Wilkins, S. W. (1996). *J. Synchrotron Rad.* **3**, 289–295.
Balaic, D. X., Nugent, K. A., Barnea, Z., Garrett, R. & Wilkins, S. W. (1995). *J. Synchrotron Rad.* **2**, 296–299.
Hoffman, S. A., Thiel, D. J. & Bilderback, D. H. (1994). *Nucl. Instrum. Methods*, A**347**, 384–389.
Kumakhov, M. A. (1990). *Nucl. Instrum. Methods*, B**48**, 283–286.
Thiel, D. J. (1992). PhD thesis, Cornell University, USA.
Wang, L., Rath, B. K., Gibson, W. M., Kimball, J. C. & MacDonald, C. A. (1996). *J. Appl. Phys.* **80**, 3628–3638.